SWITCHING OVERVOLTAGES IN A 400-KV CABLE SYSTEM

Mustafa Kizilcay
University of Siegen
Siegen, Germany
kizilcay@uni-siegen.de

Abstract – This paper deals with the computation of switching overvoltages in a 400-kV XLPE cable system that has been in service for several years. A joint failure in that cable system and recorded voltage and current wave-forms by the protective equipment that showed significant temporary overvoltages in another cable route have been the reason to analyze the switching surges in this EHV cable with shunt compensation. The cable model set up has been verified by comparison of field measurements and the digital simulations at first step. The switching surges that have been analyzed are 1) the energization, 2) deener-gization and 3) energization and subsequent deenergiza-tion of the 400-kV cable with the line-side shunt reactor. The overvoltages in the cable have been determined statis-tically by changing circuit-breaker pole closing times according to a distribution function in a statistical manner. It has been shown that in the latter case, 3), critical low-frequency overvoltages may occur, if the already energized cable will be switched off immediately by the malfunction of the protective equipment. Those overvoltages are re-lated closely to the inrush current of the shunt reactor at the moment of current interruption.

Keywords: Overvoltage, transients, EHV cable, shunt reactor, EMTP, energization, switching.

1 INTRODUCTION

The 400-kV power cable in question has been in operation for 9 years. It is one of the first XLPE cables which was put into service in European region. After several years of successful operation a fault occurred in a cable joint that had an internal problem as discovered later by a post-mortem. The cable has a length of 6.5 km. The charging current is compensated by a shunt reactor connected to the line-side, i.e. it is always switched together with the cable.

Another recent incident occurred on a different 400-kV cable route of the same transmission system has showed a necessity to analyze and review switching surges in this power system. Since the digital protective relays are installed in that 400-kV system, the wave-forms of voltages and currents are recorded by the protection at any system disturbance. A shunt compensated 400-kV line similar to the cable in question was tripped by the protection immediately after it was energized. As shown in Figure 1 the line voltage increases suddenly after the disconnection of the cable and decreases gradually with a low-frequency oscillation close to power frequency.

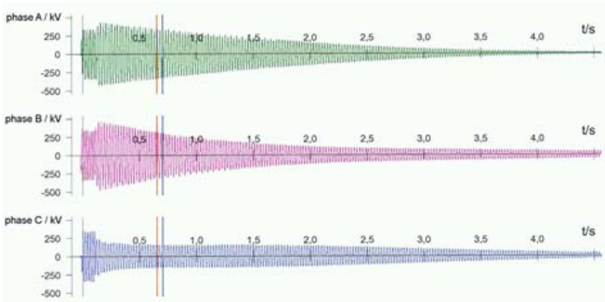

Figure 1: Recorded waveforms of the line voltages of a line (L1 in Fig. 3) energized and subsequently switched off

This observed phenomenon of switching overvoltages was important to investigate whether or not a similar case may repeat on another line and to find out the origin of the overvoltage.

2 SYSTEM MODELLING

2.1 400-kV Cable (L4)

The cable system consists of the major components a) cable tunnel, b) two parallel cable circuits – L4 and L5 in Fig. 3 – and c) grounding wire as shown in Figure 2. The tunnel runs at a depth of approx. 25 to 30 m below earth surface. Its outside diameter is 3.6 m and the inside width 3 m. The tunnel is made of precast concrete units. The location of the grounding wire in the tunnel is shown in Figure 2. The cross-section of this non-insulated copper wire is 240 mm².

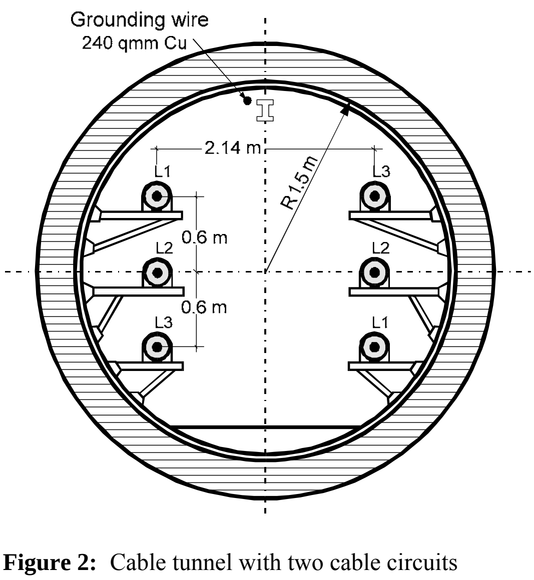

Figure 2: Cable tunnel with two cable circuits

It is connected to the metal rings mounted in the tunnel wall at every 2.4 m. Both ends of the grounding wire are grounded in the substations.

The cables are single-core (SC) XLPE cables of the type 2XS(FL)2Y 1x1600 RMS/250 220/380 kV. The screens of both cable circuits are cross-bonded; each cable system is subdivided into 3 major cross-bonding sections. Metal-oxide surge arresters ($U_r = 11.3$ kV; $U_c = 9$ kV) are installed at the cross-bonding locations across the sheath and ground. The CABLE PARAMETERS (CP) routine [5] of EMTP-ATP is used to create basic electrical parameters of the cable. CP produces directly model data for the *Constant-Parameter Distributed-Line* (CPDL) model and multi-conductor Pi-circuit component.

The cable system including the tunnel has been represented using pipe-enclosed type (PT) cable. Grounding wire has been omitted in the model. The cross-bonding of the cable sheaths is modelled in detail including the surge arresters.

Previous research [2], [3], showed that a good agreement of the simulation and measurement of the wave propagation in the 400-kV cable system can be achieved, when the semi-conducting layer (SCL) of the XLPE cable is taken into consideration in the line model. The three SC cables of the circuit in question are modelled by taking the SCL of only of the core into consideration. Presently, the CP routine does not allow representing SCL individually. Number of conductors for each SC cable is limited to three. Because the XLPE cable does not have any metallic armour, the semi-conducting layer next to the core is represented as sheath in terms of CP. A fictitious very thin insulator has to be specified between core and semi-conducting layer. The outer semi-conducting layer cannot be modelled because of the limit of number of conductors. Using bundling method known from overhead lines [4] the core and the SCL are bundled to make up an equivalent core [3]. This method is justified in [6]. The CPDL model with the consideration of the SCL is used only for the computations of cable energization. For the switching-off of the cable use of multi-conductor Pi-circuit is sufficient and reliable. None of the in [5] available frequency-dependent line models could produce satisfactory simulation results [1].

2.2 400-kV Power System

The single-line diagram of the modelled 400-kV system is shown in Figure 3. ES1 and ES2 are equivalent sources represented by a Thevenin equivalent consisting of voltage source and short-circuit impedance of the positive- and zero-sequence system. L1 to L7 are transmission lines (mostly cables; part of L1 is overhead line, (OHL)). L4 is the cable, for which the switching overvoltages will be investigated. Total length of the transmission lines is 55.9 km, the portion of the OHL is only 2.6 km. SR1, SR3, SR4 and SR5 are the line-connected shunt reactors in Y-connection and the star-point is earthed. The 400/110-kV transformers are represented in detail. The 110-kV systems are modelled in simplified form either as network sources in case of power generation or as equivalent load impedances. The system data is summarized in Table 1.

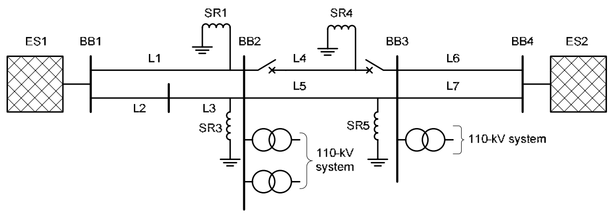

Figure 3: Single-line diagram of the 400-kV system

ES1:	V = 406.5 kV; Z_{sc} = (1.4 + j17.7) Ω
ES2:	V = 403.7 kV;Z_{sc} = (1.5 + j14.7) Ω
Line lengths:	L1: 8.1 + 2.6 km (cable + OHL); L2: 5.3 km; L3: 5.4 km; L4: 6.5 km; L5: 6.5 km; L6: 5.4 km; L7: 5.3 km
110-kV system at BB2:	5 x 200 MVA transformers; total load = 575 MW
110-kV system at BB3	3 x 250 MVA transformers; total power injection: 162 MW
Shunt reactors:	SR1: 80 Mvar; SR3: 81 Mvar; SR4: 82 Mvar; SR5: 82 Mvar

Table 1: Data of the modelled system

L4 and L5 are parallel lines in the same tunnel, which are represented in detail. The remaining lines are assumed to be balanced and represented by their impedances and capacitances of the positive- and zero-sequence systems per unit length.

The shunt reactors SR1 and SR3 have a 5-leg core and it is sufficient to model them with their positive-sequence impedance. The shunt reactors SR4 and SR5 have a 3-leg core, therefore they have been modelled by taking into consideration the positive- and zero-sequence impedance, which are not equal. Additionally, the core saturation of the shunt reactor SR4 has been represented according to a voltage-current characteristic shown in Figure 4. SR4 is connected to the cable L4 as shown in Figure 3 and plays a role in switching transients of L4.

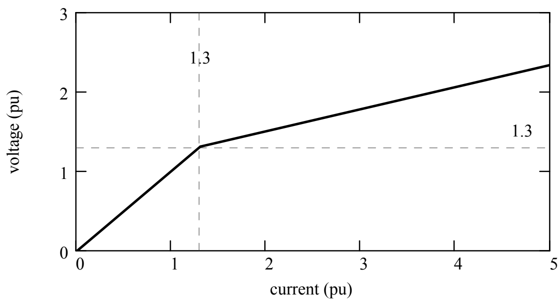

Figure 4: Voltage-current characteristics of the shunt reactor SR4 (positive-sequence system)

3 VERIFICATION OF THE SYSTEM MODEL

3.1 Available Measured Data

The transmission system operator (TSO) provided the following measured/recorded data of the line L4, which are used to verify the cable model created:

a) positive- and zero-sequence impedance and cable capacitance per unit length at 50 Hz;
b) sheath voltages and currents along the cables L4 and L5;
c) recorded voltage and current waveforms of a single-line-to-ground fault on L4;
d) Records of surge propagation field measurements performed before putting the line into service.

Using the additionally provided power flow computation of the 400-kV system, the steady-state condition of the simulation model could be adjusted.

In the following the comparison of the measurements a) and d) with the computation results will be shown exemplarily. Detailed comparison of field measurements and computations for d) can be found in [2].

3.2 Cable Impedance and Capacitance

The positive- and zero-sequence impedance are calculated by a phasor solution of EMTP-ATP, where the cable system considering the cross-bonding of the sheaths is represented by Pi-circuits in 9 sections as built. The comparison of measured and computed electrical parameters is given in Table 2.

Quantity	Measured	Computed
pos-seq. impedance (Ω/km)	0.020 + j 0.231	0.016 + j 0.219
zero-seq. impedance (Ω/km)	0.075 + j 0.079	0.103 + j 0.069
capacitance (μF/km)	0.1786	0.1786 (ε_{rXLPE} = 2.45)

Table 2: Comparison of the measured and computed electrical parameters of line L4

3.3 Surge Propagation in a Single-Core Cable

Figure 5 shows the test setup for the measurement of the propagation time and the surge impedance of one cable (phase a). To obtain the characteristic transmission line parameters of a SC cable without cross-bonding, all cross-bondings had to be removed, the corresponding cable screens along each SC cable were linked together, the sheath voltage arresters were short-circuited and earthed, and the conductors and screens of all other unused cables were earthed at both ends.

A step voltage of +30.0 V was injected between the inner conductor and screen of the cable a through a 30-Ω resistor in series with the conductor. The receiving end of the cable was open-ended. The voltage was measured at the sending end, as indicated in Fig. 5.

The measured and computed voltage waveforms are shown in Fig. 6. The voltage step which propagates through the cable can be read to 15.6 V. The reduction from 30.0 V is due to the voltage division between the 30-Ω resistor and the surge impedance of the cable. The peaks on top of the rectangular pulse are caused by the partial reflections of the travelling wave at the discontinuities of the 8 cable joints. Those spikes are reproduced in the model by small series inductances at the location of cable joints. The full reflection of the surge at the receiving cable end can be seen after the double propagation time. The shape of the reflected voltage signal is no longer rectangular due to the high frequency damping behaviour of the cable.

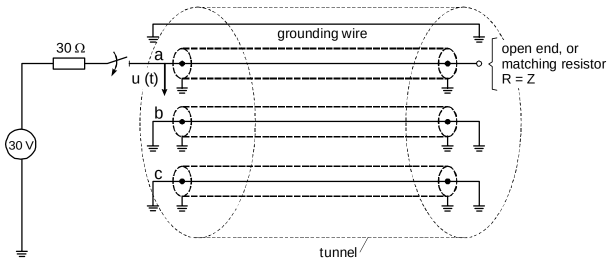

Figure 5: Field measurement to determine surge propagation characteristics

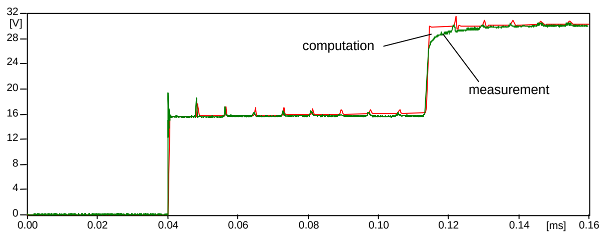

Figure 6: Measured and computed voltage waveforms at the sending end of cable L4

The analysis of the field measurements resulted in following cable surge parameters:

– surge impedance: 32.69 Ohm
– travel time: 36.52 μs
– propagation velocity: 179.24 m/μs.

4 SWITCHING OVERVOLTAGES

4.1 Energization of the Uncharged Line L4

Various system parameters that may effect the switching surges and hence overvoltages of line L4 are taken into consideration in the computations. They are:

– model of the cable system (L4 and L5);
– linear and nonlinear shunt reactor model;
– energization from both ends of the line;
– random closing of the circuit-breaker (CB) poles (statistical analysis of switching overvoltages).

As line model CPDL of [5] is used, which is the well-known Bergeron traveling wave model. Model parameters are determined at f = 7 kHz, which is approximately the fundamental resonant frequency of the open-ended SC cable. A comparison of switching transients is made for two alternatives of the cable system modelling: a) Cable L4 is represented independently without considering the coupling to the parallel line L5;

effect of the SCL is taken into account; b) The whole cable system consisting of L4 and L5 is modelled, but the SCL is omitted, i.e. taken as part of the conductor. The voltage waveforms at the receiving end (BB2) are shown for both cases in Figure 7, when the cable is energized from BB3 end at voltage maximum of phase *a*. No significant difference in the waveforms can be seen in Figure 7.

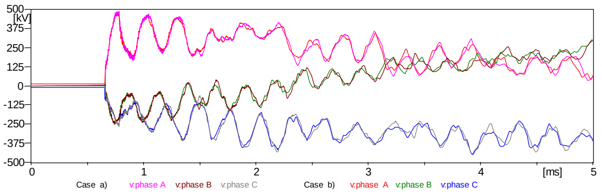

Figure 7: Voltages at the receiving end; comparison of line model alternatives a) and b)

As can be expected, the linear and nonlinear model of the shunt reactor has practically no influence on the voltage waveforms. However, the terminal, from which the line is energized, has an influence on switching transients due to the location of the shunt reactor (SR4). The influence of the location of SR4 on overvoltages is rather small as it can be depicted by the statistical analysis of switching overvoltages.

A statistical analysis of energization overvoltages is performed using STATISTICS switch [5] to model the random mechanical pole spread. The first pole (phase *a*) to close is taken as master switch that will close according to the uniform distribution within a half cycle, i.e. 10 ms. The other two poles close with a maximum pole spread of 3 ms according to the uniform distribution as slave switches. Total 200 simulation runs were performed for an energization study. The probability of overvoltages corresponding to a certain overvoltage factor *k* and greater can be read from the cumulative frequency curves in Figure 8.

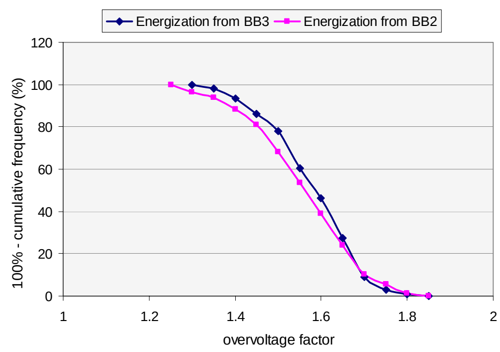

Figure 8: Cumulative frequency distributions of overvoltages at the receiving end for the energization of L4 from both ends

The overvoltage factor for line-to-ground voltages is defined by the following equation:

$$k = \frac{|v_{peak}|}{\frac{\sqrt{2}\cdot 380\text{ kV}}{\sqrt{3}}} = \frac{|v_{peak}|}{310.27\text{ kV}} \qquad (1)$$

The maximum overvoltage factor amounts to 1.83. Slightly greater overvoltages are expected, if the line is energized from the end at BB3, where SR4 is located.

Additionally the energy absorption of sheath surge arresters at cross-bonding locations is statistically analyzed. The greatest thermal stress by overvoltages is expected at the cross-bonding point nearest to the energization end, where SR4 is installed. The energy absorption of the surge arresters is uncritical during energization, however.

4.2 Switching-Off of the Line L4 in Steady-State

The disconnection of the cable L4 in normal operation does not cause any critical overvoltages. After the second CB has opened, the voltage on the line decreases gradually with a low-frequency of 56 Hz resulting from the inductance of the shunt reactor and the cable capacitance. The voltage waveforms after disconnection of the cable at 20 ms are shown in Figure 9.

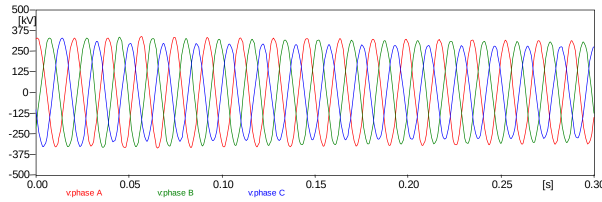

Figure 9: Voltage waveforms of the disconnected line L4

4.3 Energization and Subsequent Deenergization of the Line L4

As it has been observed on line L1 (see Figure 1), a sudden voltage rise may occur on a shunt compensated line, when after energization the line will be tripped immediately by the protective relay. This phenomenon has been analyzed in detail in this study. Particularly, it is important to know under which conditions a critical overvoltage may occur and what will be its amplitude in the worst-case.

In steady-state the no-load current (one end open) of the line L4 compensated by the shunt reactor is only 22 A (inductive current). When the line together with the SR4 is energized, a typical unsymmetrical inrush current flows into the SR that may go into saturation depending on the magnetization curve and the instant of switch closing. The inrush current of the SR continues to flow several cycles. When the line will be disconnected at an instant, as the inrush current in one of the phases is maximum, then a high overvoltage occurs along the line after switching-off, because that inductive current tends to flow through the cable capacitance, which is the only remaining current path. The line capacitance establishes a high impedance path for this current, consequently the line voltage increases. This phenomenon is illustrated by means of digital simulations. The line is energized at the instant of voltage maximum of phase *a* from the BB3 end (see Figure 10) and approx. 80 ms after energization it is disconnected at the instant as the current (phase *c*) of SR4 is maximum (Figure 11). The vertical dotted line in Fig. 11 shows the instant of opening of the last CB pole. Line-to-ground voltage of phase *c* increases up to $k = 2.4$ p.u. as it can be seen in Fig. 10.

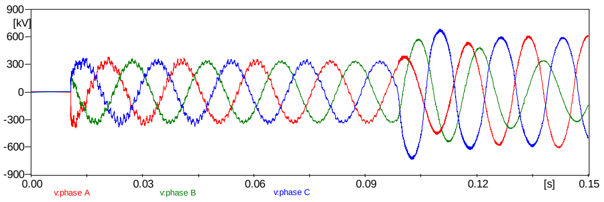

Figure 10: Waveforms of the line-to-ground voltages at the BB3 end resulting from energization and deenergization at the maximum of SR current in phase *c*

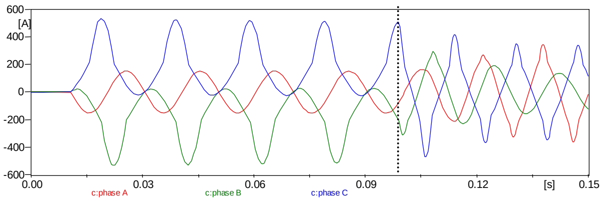

Figure 11: Waveforms of the shunt reactor (SR4) current during energization and deenergization at the maximum of SR current in phase *c*

Another simulation should illustrate the harmless case with no overvoltage, when the line is disconnected at the instant of minimum shunt reactor current. The corresponding waveforms of the line-to-ground voltage and the shunt reactor current are shown in Figures 12 and 13, respectively.

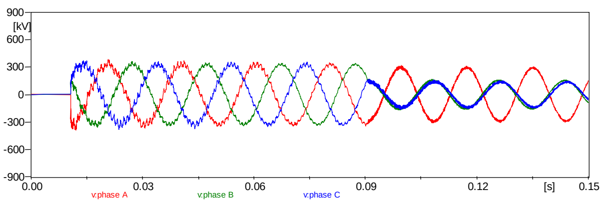

Figure 12: Waveforms of the shunt reactor (SR4) current during energization and deenergization at the minimum of SR current

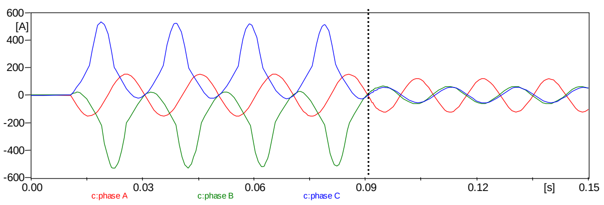

Figure 13: Waveforms of the shunt reactor (SR4) current during energization and deenergization at the minimum of SR current

Since the waveforms of the SR current are dependent on the instant of switch closing and the overvoltages result from the switching-off instant, it is convenient to perform a statistical analysis to determine cumulative frequency distribution of the overvoltages. This time two three-phase STATISTICS switches are required; one for the closing operation and the second one for the opening. The maximum pole spread for opening is given by the CB manufacturer as 2 ms. The closing and opening times are determined randomly according to the uniform distribution. Total 250 simulation runs are performed for this statistical analysis. The cumulative frequency distribution of the overvoltages at the receiving end is shown in Figure 14 for the energization and deenergization of the line L4 from both ends. The average time difference between energization and deenergization is set to 4 cycles (80 ms). The maximum overvoltage amounts to $k = 2.6$ p.u. The overvoltages on the line are slightly greater, if L4 is energized and deenergized from the BB3 end, where SR is located. These overvoltages of low-frequency are still smaller than the specified line-to-ground switching impulse withstand voltage for the 400-kV equipment. The sheath surge arresters of the line L4 are not stressed critically by the energization and deenergization transients. The energy absorption is fairly below the rated value.

The shunt reactor was modelled with a nonlinear magnetizing characteristic in the above computations. It has been further investigated that a linear shunt reactor may also cause high overvoltages. The overvoltage amplitudes in this particular case are about 7 % lower.

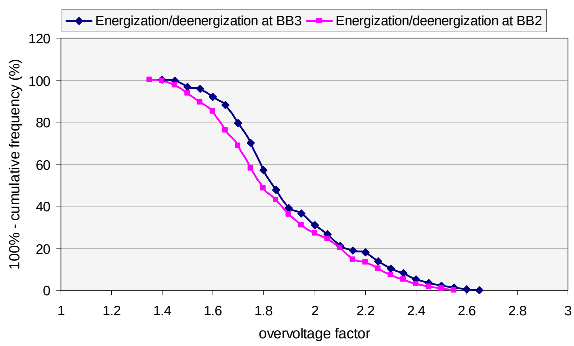

Figure 14: Cumulative frequency distributions of overvoltages at the receiving end for the energization/deenergization of the line L4 from both ends

5 CONCLUSION

Switching overvoltages in an existing 400-kV cable system consisting of XPLE cables are studied by means of digital transient computations. Two incidents in the system operation gave rise to this detailed study of switching transients in a particular 400-kV cable.

The system model created has been verified by the available field measurements and transient records. The comparison of the computations and measurements showed a good agreement of the results.

Statistical analysis of switching transients showed that the energization and deenergization of the shunt compensated 400-kV cable do not cause critical overvoltages and high thermal stress on the sheath surge arresters. The influence of the line-side shunt reactor on the overvoltages during energization is insignificant.

Energization and subsequent deenergization of a cable with a shunt reactor connected to it may cause high overvoltages depending on the instant of energization, hence the inrush current built in the shunt reactor and on the instant of disconnecting the line, hence the instantaneous value of the inrush current at the switching-off instant. The ability of the circuit-breaker to interrupt the currents of the just energized line/cable and of the shunt reactor depends also on the compensation degree. If the just energized line/cable is switched-off at the instant of maximum current of the shunt reactor, a high overvoltage is to be expected along the line. It is due to the fact that the inductive current tends to flow through line capacitance causing high voltage drop over it. This phenomenon may happen generally on all shunt compensated lines depending on the degree of the compensation and amplitude of the inrush current as it occurred once in the 400-kV system investigated.

REFERENCES

[1] M. Kizilcay, M. Ermel, S. Demmig, H. Biewald, “Modelling of a 400-kV XLPE cable system”, Proceedings of the EEUG Meeting 1999, Gizzeria Lido, Calabria/Italy, November 1999.

[2] M. Kizilcay, M. Ermel, S. Demmig, “Computation of surge propagation in a 400-kV XLPE cable by taking the inner semi-conducting layer into consideration”, EEUG Meeting 2000, Wroclaw, Poland, September 2000.

[3] M. Kizilcay, “Modelling of a 400-kV XLPE cable by taking into consideration the semi-conducting layer of core”, European EMTP-ATP Conference, UWE Bristol, UK, September 2001.

[4] Bonneville Power Administration, “EMTP Theory Book”, Branch of System Engineering, Oregon, USA, 1987.

[5] Canadian/American EMTP User Group, “ATP Rule Book”, Portland, Oregon/USA, revised and distributed by the EEUG Association, 2006.

[6] A. Ametani, Y. Miyamoto, N. Nagaoka, “Semiconducting layer impedance and its effect on cable wave-propagation and transient characteristics”, IEEE Transactions on Power Delivery, Vol. 19 (2004), H. 4, S. 1523-1531.